SSC24-WVI-03

Development and Results of a Lasercom Testbed for the CLICK B/C CubeSats and Future Missions

Thomas S. Schwarze, Danielle E. Coogan, Joseph Conroy, Pablo Santiago, John W. Conklin
Department of Mechanical and Aerospace Engineering, University of Florida,
Gainesville, FL, USA
t.schwarze@ufl.edu

Myles Clark
Max Planck Institute for Gravitational Physics (Albert Einstein Institute) and
Institut für Gravitationsphysik, Leibniz Universität Hannover,
Hannover, Germany

Paul Serra, Hannah Tomio, Nicholas Belsten, William Kammerer, Celvi Lisy, Paige Forester, Mohamed Mohamed, Leonardo Gallo, Ajay Gill, Kerri Cahoy
Department of Aeronautics and Astronautics, Massachusetts Institute of Technology,
Cambridge, MA, USA

Jan Stupl, David Mayer
NASA Ames Research Center,
Mountain View, CA, USA

John Hanson
CrossTrac Engineering,
Mountain View, CA, USA

ABSTRACT

The expansion of interest in small satellite constellation networks underscores the need for precise timing synchronization and reliable high-bandwidth communication between spacecraft. The CubeSat Laser Infrared CrosslinK (CLICK) mission is being developed by the Massachusetts Institute of Technology, the University of Florida, and NASA Ames Research Center. The first phase of the mission, CLICK A, was launched on July 14, 2022, aboard SpaceX's CRS-25 and put into orbit from the International Space Station, where it successfully demonstrated the downlink to Earth. The second phase of the mission (CLICK B/C) will additionally demonstrate a crosslink between two 3U CubeSats (B and C) that each host a 1.5 U laser communication payload. The terminals will demonstrate full-duplex spacecraft-to-spacecraft communications and ranging capability using commercial-off-the-shelf components at low size, weight and power (SWaP). As part of the mission, CLICK will demonstrate two-way time transfer for chip-scale atomic clock (CSAC) synchronization and data transfer. This data transfer will use pulse-position modulation (PPM) at rates between 20 Mbps and 50 Mbps over separation distances ranging from 25 km to 580 km. A time-transfer precision of < 200 ps between the spacecraft is targeted. CLICK B/C is scheduled to launch in 2025. The University of Florida hosts a testbed to support CLICK developments. Its goal is to enable testing of the optical data- and timing-transfer chain on ground. This encompasses the vital components of the CLICK hardware for both TX (transmission) and RX (receiving). For TX, the electronics and laser system to generate optical pulses are included, with the latter consisting of a micro-integrable tunable laser assembly as seed laser and a semiconductor optical amplifier as shutter. In turn, the RX side consists of an avalanche photodetector (APD) to capture the pulses, electronics to condition and convert the analog signal into the digital domain (time-to-digital and analog-to-digital), and a field-programmable gate array as DSP (digital signal processing) platform. The DSP implements the algorithm to decode the PPM scheme and extract timing information. In between the optical TX and RX, an electrical variable optical gain amplifier is placed to simulate varying distances between satellites and the associated change in received power. The final setup is envisioned to use separate hardware platforms for TX and RX to test the timing transfer between independent CSACs. Here we present the status of the testbed and the associated development of CLICK hardware and DSP, in particular the APD and PPM decoder, along with results of the lasercom testing, showing initial tracking of test data.

Introduction

Space missions and their satellites continue to demand increased data bandwidth, as the number and data output of deployed instruments grow. Constellations and autonomous swarms of satellites require rapid exchange of data, ranging, and timing information between their nodes.[1] This leads to the need for efficient and high-bandwidth communication, precision time-transfer, and ranging. While high-speed radio frequency (RF) links are the state of the art, laser crosslinks have been identified as a promising path to address high bandwidth needs and have been developed over three decades.[2,3]

For data transfer, laser communication (lasercom) pushes into new domains of bandwidth. In contrast to conventional RF communication, lasercom operates at orders of magnitude higher carrier frequencies, in the THz regime. This enables faster modulation and hence higher data rates. Likewise, divergence and associated power loss are significantly reduced, enabling systems with lower size, weight and power (SWaP). On the other hand, the narrower beams lead to more challenging pointing requirements. Recent mission demonstrations have emphasized the potential of lasercom. The TeraByte InfraRed Delivery (TBIRD) mission demonstrated downlink rates in the 100 Gbps range and the Lunar Laser Communications Demonstration (LLCD) and Deep Space Optical Communications (DSOC) missions showed the feasibility of laser-com for deep-space communication.[4,5,6]

The role of the CubeSat Laser Infrared CrosslinK (CLICK) mission is to demonstrate miniaturization of a laser link between two spacecraft with commercial-off-the-shelf components (COTS) and low SWaP for data communication, time-transfer and ranging.

CLICK is divided into two phases, CLICK A and CLICK B/C. The former is a risk reduction mission which was launched in 2022. CLICK B/C will consist of two 3U CubeSats (B and C), each with 1.5 U lasercom payloads and a targeted weight and power budget of 1.5 kg and 30 W, respectively. For the demonstration of intersatellite data transfer, timing and ranging, CLICK B and CLICK C will be transmitting 1565 nm and 1537 nm laser beams, respectively. Targeting full-duplex transfers, both spacecraft are equipped with avalanche photodetectors (APDs) to detect the laser light with high efficiency and each spacecraft can act as both transmitter (TX) and receiver (RX). The data and time-transfer scheme is pulse position modulation (PPM). CLICK B/C are designed to support data transfer at spacecraft distances from 25 km to 580 km, with data rates of 50 Mbps and 20 Mbps, respectively. Timing precision of < 200 ps is also targeted.

The testbed at University of Florida (UF) is focused on the data and time-transfer scheme and associated hardware components. This paper describes the flatsat under development to provide a testbed for the components used in CLICK as well as to serve in the future to continue to evolve techniques and components.

First a general description of the CLICK mission concept, including its risk reduction mission CLICK A, will be given. Subsequently, key components will be described in more detail. Finally, the plan for the UF testbed, its current status and preliminary results are presented.

CLICK OVERVIEW

Except for the emitted laser wavelengths (1565 nm, 1537 nm), the two CLICK satellites are symmetric. Their 1.5 U payloads consist of an optical bench and the avionics. The main challenges are the pointing, acquisition and tracking (PAT) of the two satellites to orient their beams to each other and the ground station, as well as the electronics to support data and timing communications once a link is established.

The full laser crosslink is shown in Figure 1. On the TX side, there are TX electronics as well as TX optics. The former are responsible for converting payload data into electrical pulses, which in turn are converted into optical pulses by the latter. TX processing is primarily implemented in a central field-programmable gate array (FPGA) and will be discussed in detail in its dedicated section. The TX optics utilize a micro-integrable tunable laser assembly (uITLA) as seed laser, reaching powers of up to 60 mW. Its continuous-wave (CW) beam is propagated through a semiconductor optical attenuator (SOA), which serves as a shutter driven by the electrical pulses. The sequenced pulses subsequently exit the active medium of an Erbium-doped fiber amplifier (EDFA). The amplified pulses are then sent out through the main telescope. Depending on absolute spacecraft distance, a certain fraction of the power is detected on the RX spacecraft. Its RX optics primarily consist of a telescope and an APD board. It converts the optical pulses back into the electrical domain.[7] The RX electronics consists of signal conditioning like amplification and digitiza-

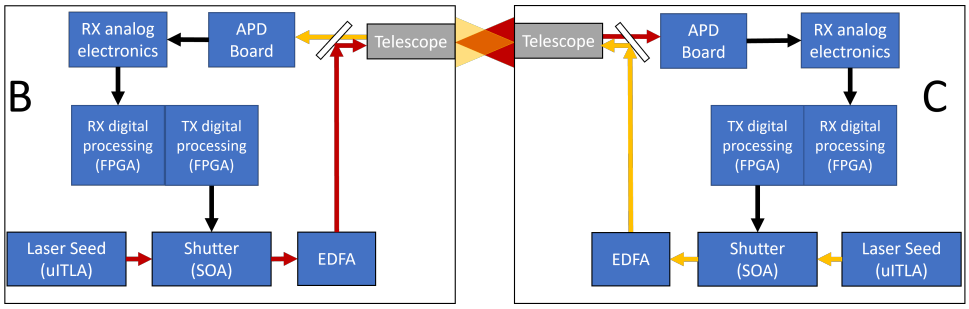

Figure 1: Schematic of the full laser data crosslink.

tion and a digital PPM decoder hosted in the central FPGA. On each spacecraft, a chip-scale atomic clock (CSAC) provides the time reference.

There are basic link budget relationships to consider. Higher data rates require reduced intervals between pulses, meaning the EDFA inversion build-up is shortened and hence less power can be transmitted per pulse, effectively decreasing signal-to-noise ratio (SNR).

A larger distance between spacecraft reduces the SNR as well. Accordingly, data rates must be adapted to compensate for this loss of SNR due to changing distances. While the RX analog conditioning electronics cannot change the SNR, they are used to condition the incoming signal to fit dynamic range of the digitization electronics.

A key capability for successfully establishing the laser link is precision PAT. The procedure for the inter-satellite PAT is divided into multiple stages. After initial positioning with the support of GPS, a 976 nm beacon laser is utilized for coarse pointing. It will be detected in the other spacecraft by a CCD camera and its centroid information will be used to adjust the spacecraft attitude. After that, fine pointing is conducted by using a quadcell photoreceiver and a micro-electromechanical system (MEMS) fine steering mirror (FSM). Figure 2 shows an overview of the optical bench of one of the CLICK spacecraft. The green lines symbolize both outgoing and incoming beacon laser light. The latter shares most of the propagation path towards the quadcell (through L1, L2 and reflected by the FSM) with the TX (red) and RX (yellow) laser beams. Adjusting the pointing for the beacon also adjusts the pointing for the TX and RX beams. Dichroic mirrors are used to separate the various beams.

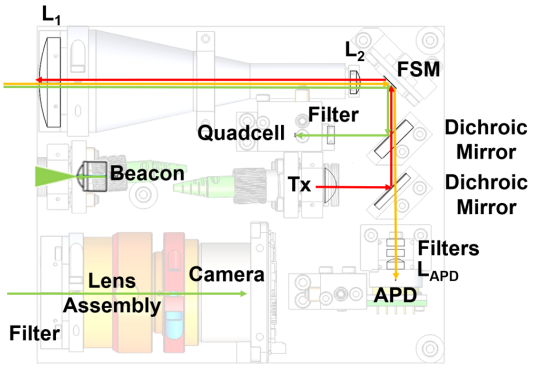

Figure 2: CLICK B/C principal optical bench design.[8]

CLICK A

Essential technology for CLICK B/C was tested with the precursor and risk reduction mission CLICK A. It comprised a single CubeSat, which was launched on July 14th, 2022, aboard SpaceX's CRS-25 and was released into orbit from the International Space Station on September 6th, 2022. The primary goal of CLICK A was to establish a first laser downlink to the ground station, which primarily puts the PAT system of both satellite and ground station to a test. Some technology shared between CLICK A and its successor mission CLICK B/C was used, namely a MEMS FSM, a silicon CMOS camera including a camera lens assembly and an EDFA. During its mission time on orbit (initially 51.6° inclination, 414 km altitude), CLICK A overpassed the ground station (Westford, MA) several times and multiple downlink attempts were conducted. An average RMS pointing error of 0.175 mrad was demonstrated. This included the compensation of a maximum spacecraft blind pointing error of 8.494 mrad. More details and description of the CLICK A spacecraft and ground station architecture can be found in the References.[9]

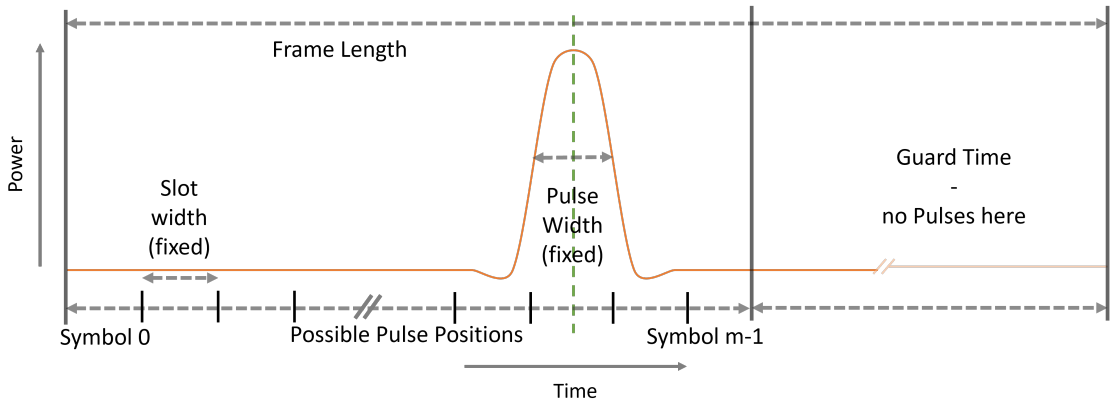

Figure 3: Illustration of a pulse within a PPM-m scheme.

CLICK DATA AND TIMING TRANSFER

The lasercom data communication is based on PPM. This means a certain number of bits b will be merged into a single symbol, which in turn is encoded by asserting a pulse in one of m possible time slots. In order to cover all possible values of b, the following relationship needs to be fulfilled:

$$m = 2^b \tag{1}$$

The number of time slots m also denotes the PPM order. With m being the main parameter, the parameters slot width, pulse width and guard time also determine the overall PPM frame. Figure 3 shows a graphical description of a PPM frame. The guard time, during which no pulses are allowed, is applied to facilitate synchronization between TX and RX, to ensure sufficient processing time for the decoding, and to provide additional power build-up for the optical pulses.[10] Slot width and pulse width are set to adjust data rate, error rate, and timing precision. The current implementation uses a fixed slot and pulse width of 10 ns. This gives a theoretical maximum of 50 Mbps, assuming PPM order 2 and two slots of guard time.

PPM decoding is of research interest. In the CLICK mission, the plan is to utilize two fundamentally different schemes for the decoding of the PPM pulses. Each scheme can be altered for different variances. The two base approaches are implemented via two distinguished electronic hardware chains, one is based on a fast analog-to-digital converter (ADC), and the other is based on a time-to-digital converter (TDC).

The basic idea of the ADC-based approach is to sample a high-resolution time series of the pulses and apply a matched filter to it. The matched filter will compare the input with the different possible pulse positions and compute correlation coefficients. This way, the correct position can be determined, and the data derived. In the second approach, a TDC is used to generate a time stamp for the time of arrival of the pulse center. The time stamps of the pulse trains are then fed to a decoder which matches them to a local RX PPM frame and its slots.

Without getting into a more detailed discussion about the advantages and disadvantages of the decoding schemes, it should be pointed out that the TDC method is more efficient in terms of taken samples: it only needs to sample and process data when an actual pulse is captured. In contrast, the standard ADC approach needs to continuously sample at the high-speed rate required to properly resolve the pulse edges, meaning that only a fraction of the samples are actually carrying useful information.

TDC-Based PPM Decoding

In this paper, the emphasis is put on the TDC approach. Its analog and digital signal processing chain will be described in detail. The concept is to condense the pulses into a single time of arrival. The incoming pulses are conditioned to trigger four distinguished rising edges, two during pulse buildup, and two during pulse settling. These edges are subsequently used to trigger four separate TDC channels to generate four time stamps. Figure 4 shows an illustration of this concept, while Figure 5 shows a schematic of its implementation in term of analog signal processing.

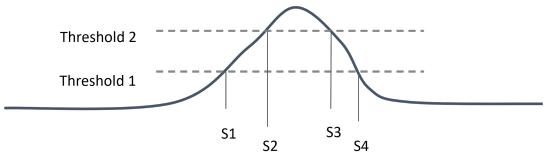

Figure 4: Illustration of pulse time stamping. Threshold 1 and 2 are the settable voltage levels at whose crossing (rising or falling) the TDC chain is triggered to generate the time stamps S1, S2, S3 and S4.

The signal captured from the APD is converted into the electrical domain, and conditioned by a set of programmable gain amplifiers (PGAs). These PGAs are responsible for adapting the signal levels to the digitizers' dynamic ranges. Subsequently, the signal can either be fed into the ADC or the TDC processing chain. Each chain starts off by applying adapted low-pass filters. While the ADC chain then digitizes the signal, the TDC chain requires further signal conditioning. First, the signal is fed into two separate comparators, each configured with a different threshold level. This means their respective outputs are asserting and de-asserting at the different signal levels of the pulses. These outputs are then each fed into two edge detectors. One of them is set to trigger on a falling edge, the other set to trigger on a rising edge. This way, triggers are generated both during buildup and settling of the laser pulses. The resulting four rising edges (shifted in time) are fed to the four-channel TDC. The TDC generates time stamps for the four events, which it then transmits to the FPGA. The time stamps processed in the FPGA are defined as ticks of a local reference clock and ultimately come with a resolution of 4.88 ps and a 64 bit dynamic range.

Within the synthesizable logic of the FPGA, the four time stamps are averaged to give a precise measure of the pulse arrival time and are subsequently fed to the digital PPM decoder unit. The decoder unit can be thought of as a delay-locked loop matching the local version of the PPM frame to the incoming train of time stamps. A convenient way to understand its functionality is to separate its two operation modes: locked state and acquisition.

Figure 6 shows a schematic of the decoder in locked mode. The starting times T_0 of the local frames with length T_{frame} are tracked in an accumulator (top left), whose value is subtracted from the incoming time stamps. Assuming locked mode and matched frames, this difference, called T_m, together with a given slot width, enables the Symbol Decoder to derive the slots of the associated pulses. It reports the decoded symbol as received data. The Symbol Decoder will also utilize the ideal time T_{m_ideal} of the determined slot and subtract it from the actual measured time T_m, resulting in an error signal T_{err}. The error signal yields information about timing jitter of the incoming signal and is utilized as an additional output. Simultaneously, it is used in a Controller as input to a custom Error Function and is further processed with a Control Law. The resulting actuation signal T_{act} is fed back and added to the output of the accumulator tracking the local frame. This way, timing drifts within the bandwidth of the Controller can be compensated for and the Symbol Decoder is kept in lock.

Figure 7 shows a schematic of the decoder in acquisition mode. In this mode, the incoming time stamps initially have an arbitrary relation to the local T_0. For pseudo-random binary sequence (PRBS) data, one of the incoming symbols will eventually be calculated by the Symbol Decoder to fall into the guard time. The Symbol Decoder will then assign the pulse to the closed valid slot, leading to an error signal T_{err} bigger than half a slot width. The Error Function is designed such that for errors bigger than half a slot width, a high gain is applied to adjust the local frame quickly. Accordingly, the local frame is adapted by the actuator signal T_{act} until no more symbols fall into the guard time. While acquisition is achieved eventually for random data, for repetitive symbols, the PPM decoder would not be able to converge on the correct symbol. On the other hand, convergence is achieved quickly for a sequence alternating between lowest and highest symbol. Hence, it is beneficial to prepend payload data with a preamble composed of such a sequence.

The current implementation runs the PPM decoder logic at 100 MHz. For the theoretical maximum speed of one pulse per 40 ns (see above), this leaves only four taps for processing.

PPM Encoding

The encoding of data into a PPM scheme is implemented on the FPGA as well. The first processing step is the division of the raw payload bytes into bit words or symbols according to the chosen PPM order. Afterwards, these need to be translated into a bit vector representing the timeline of the pulses in binary, dependent on slot and pulse width. The timeline in turn is used to feed the Serializer/Deserializer (SerDes) TX of the FPGA, converting it into the analog domain with a resolution of 500 ps.

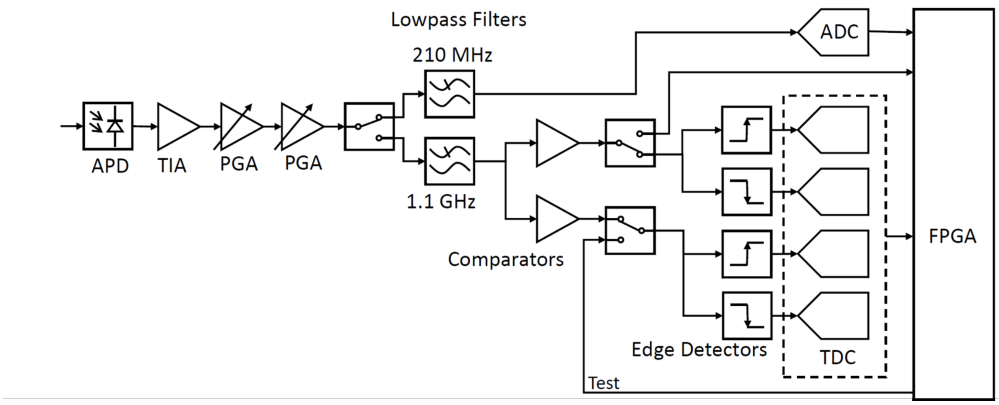

Figure 5: Schematic of the analog signal processing for the ADC and TDC chain.

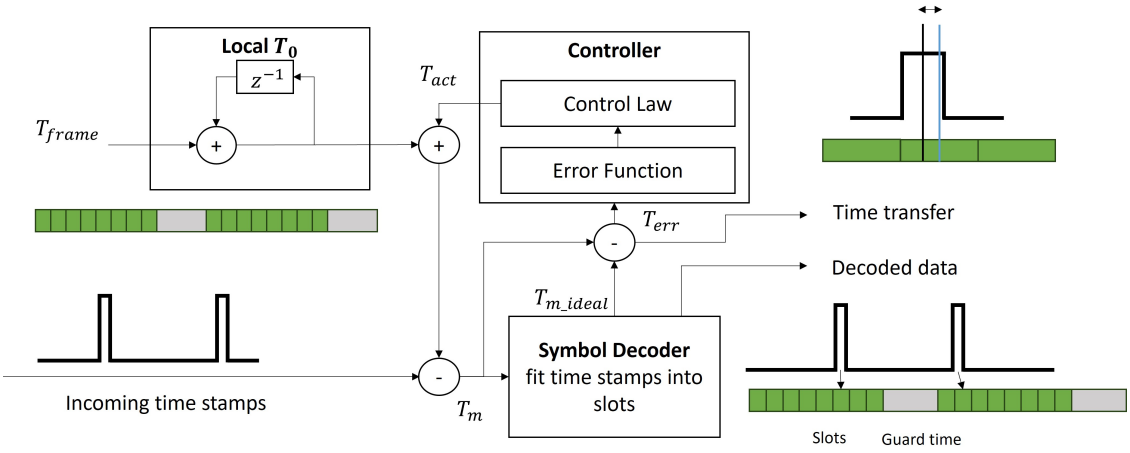

Figure 6: PPM decoder in locked mode. Incoming time stamps are transferred into the local time frame by subtracting the local T_0. Afterwards they are fitted into a valid slot to obtain the payload data. Deviations from the ideal slot center are fed to the Controller to keep the local frame in lock. The error also serves as time-transfer measurement.

APD BOARD

To achieve power efficiency for the laser link, a crucial component is the sensor. The CLICK mission utilizes APDs. Such devices use the avalanche effect to yield a high sensitivity to even small amounts of incoming photons. It is a photodiode that is optimized for and operated with a high reverse voltage bias. Once impinging photons generate free electrons through the photoelectric effect, these are strongly accelerated by the high bias and can generate further free electrons by collision. Collectively, both groups are accelerated once again and can free even more electrons, ultimately leading to an avalanche effect. The APD comes with a transimpedance amplifier (TIA) and is hosted on a custom PCB, called the APD board. It consists of a signal conditioning chain, subsequent to the APD, and interface electronics, as shown in Figure 8. The signal chain of the APD board is equipped with two consecutively placed differential PGAs. Each of them provides an attenuation/amplification range of -6 dB up to 26 dB. The purpose of the PGAs is to be able to adapt to the changing input power due to changes in spacecraft distance. While this will not change the SNR, it is important to utilize the full dynamic range of the subsequent ADCs and TDCs. The interface electronics of the APD board make the manifold control settings accessible for read and write by the digital control system via serial peripheral interface (SPI) and a slow ADC/DAC. The PGAs can be controlled directly via SPI, while other parameters like APD bias need to be set via the ADC/DAC, which in turn is interfaced via SPI.

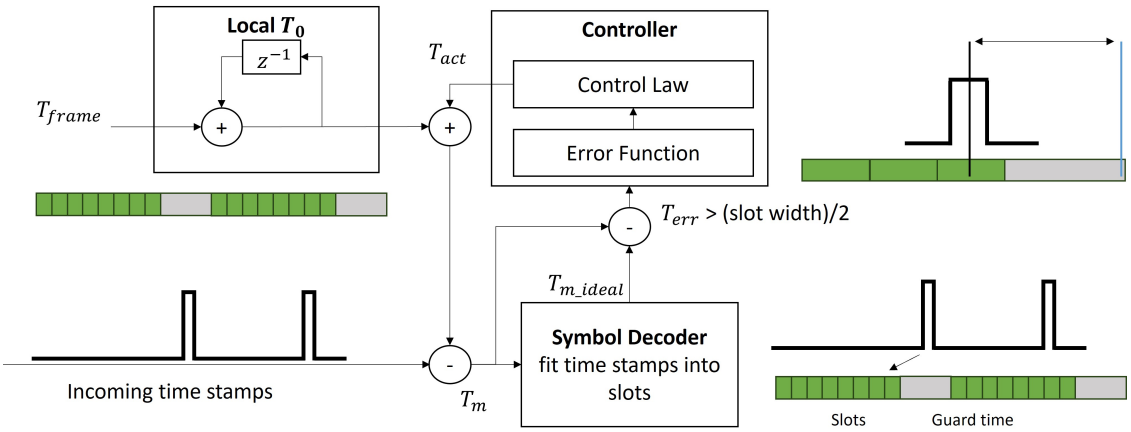

Figure 7: PPM decoder in acquisition mode. By design of the Error Function, those time stamps that fall into the local guard time generate a strong actuation signal. This eventually matches the local time frame to the incoming time stamps.

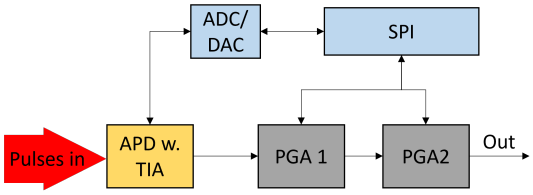

Figure 8: Schematic of APD board.

UF TESTBED

The University of Florida is developing a flatsat setup to both serve as ground support equipment (GSE) testbed for the CLICK B/C mission and to advance the technology development for future missions.

Goals

The goal of the UF testbed is to establish an optical link between two independent instances of hardware, emulating the two CLICK B/C CubeSats. This enables testing the data laser link between two unsynchronized units, and in particular, the measurement of timing noise between two independent CSACs. To focus on these aspects, the challenges of PAT are not addressed with this testbed.

Configuration

Figure 9 shows a schematic of the different milestones for the UF testbed. The primary difference between this and the flight hardware is the lack of the PAT, lack of an EDFA, and the addition of a variable optical attenuator (VOA). The latter aims to simulate the changing power levels due to satellite distance changes and different PPM orders.

In a first step, a single optical link will be established, using a single avionics unit communicating with itself in an optical loopback configuration. Only a single CSAC will be used. In the second step, two avionics units will be deployed, one acting as TX and the other as RX. Both will be driven with independent CSACs. In the third step, a second optical link will be established, enabling both platforms to act as both TX and RX for a full duplex link.

Implementation Progress

The initial flatsat operates in a preliminary fashion with limited features. Figure 10 shows a schematic of its status. It tests the two main components of interest, the APD board and the TX-RX system, separately. This is because the SOA still needs to be integrated, as it is required to convert the electrical signal from the FPGA into the optical domain.

As a makeshift solution for testing the APD board, a laser diode which can be pulsed directly with a signal generator has been used. While the APD board is still operated by the FPGA, its output signal is currently monitored with an oscilloscope for analysis and characterization.

For the testing of the TX-RX system, the optical loopback is replaced by a simple electrical loopback, meaning the pulses generated by the FPGA are bypassing any optical devices and are fed straight back into the RX input. While the next iteration of hardware is being fabricated, only one TDC channel is used. The CSAC is not yet implemented.

Despite the reduced functionality of the setup,

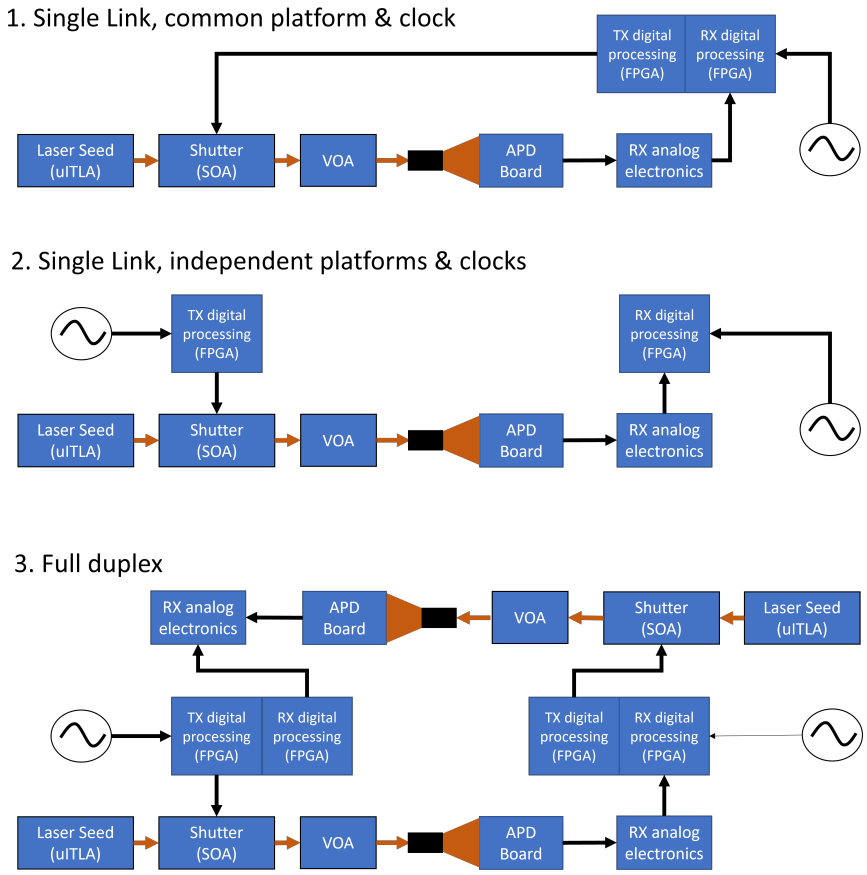

Figure 9: Different milestones of the UF testbed.

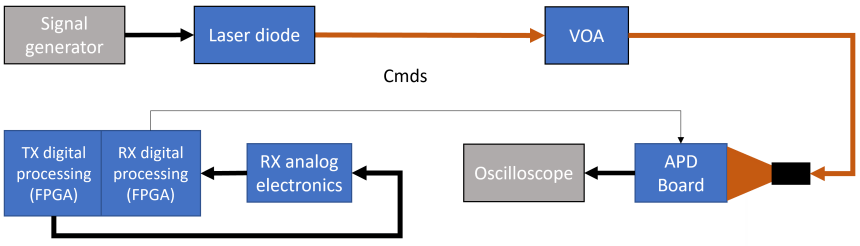

Figure 10: Current configuration of UF testbed, working towards milestone 1 in Figure 9.

important testing results are obtained, such as first functional tests of the TX-RX system and the APD board.

Data Transfer Electrical Loopback Preliminary Results

The current testbed has enabled the testing of the analog and digital TX and RX units via an electrical loopback. In first tests, proof of principle measurements were successfully conducted. These consisted of the transmission of a simple pattern alternating between maximum and minimum PPM symbol. As mentioned, such a pattern is envisioned as a preamble for actual payload data and is meant to help the PPM decoder adjust its local time frame. In the preliminary tests, the preamble pattern could be successfully captured by the decoder. Different PPM parameter sets were tested. Table 1 shows examples of parameter sets of a preliminary test run. Parameters that are varied besides the PPM order include guard time, frame length, and an attenuation (negative gain) applied to T_{act} .

Table 1: Loopback test with preamble only. Sample size: 16384.

PPM order	Guard time (ns)	Frame length (ns)	Gain (dB)
2	80	120	-12
3	40	120	-12
4	40	200	-6
6	210	850	0

While these results require a proper statistical verification, they serve as a first system check. One observation that can be made is that lower PPM modes obtain better results with higher attenuation compared to slower PPM modes. PPM mode 5 data was omitted due to a software issue, this will be addressed in future work.

In a next step, random data is appended to the preamble to simulate payload data. The decoder shows the ability to track random data succeeding the preamble for 2k symbols, however the initial test run had a higher bit error rate than expected, and correcting this is also an area of future work.

Primary criteria for testing the APD board are its amplitude noise contributions and the added timing jitter for incoming pulses.

For investigation of the added jitter, the latest version 4.3 of the APD board was available. The laser diode was pulsed with the external signal generator and the oscilloscope monitored the APD board's output. The testing showed timing jitter exceeding the required performance. However, the jitter contains both laser source and APD board contributions, which could not be disentangled at this point. Assumptions are that the main jitter source is the laser. This hypothesis will be verified when installing the uITLA and SOA system. Until then, the test serves as a rough functional test.

An extensive characterization of amplitude noise was conducted for the predecessor version 4.2 of the current APD board.[11] Only minor changes were made between versions. Figure 11 summarizes the investigation. The optical setup as shown in Figure 10 is used for the testing, but with either continuous or no laser light applied. The blue line shows the noise equivalent power (NEP) of the APD board output under illumination by approximately 0.33 W of power. The red line shows the NEP without light, representing the dark current. Except for spikes around 2 and 4 MHz, the NEP under illumination fulfills the CLICK B/C requirement of 15 pW/sqrt(Hz).

Summary and future work

CLICK B/C is in the final stages of the CLICK project, which started with the development of CLICK A and its launch as a risk reduction mission in 2022. CLICK will demonstrate lasercom between two CubeSats with low SWaP and utilizing COTS components. The University of Florida has set up a testbed to demonstrate and investigate key elements for the mission. This includes the laser link for lasercom, timing transfer and ranging, and optical hardware elements like the APD. It is not intended to test the PAT with this testbed. The final setup will feature a full duplex link. The current status is at an initial stage with an electrical loopback test and a separated laser source for APD testing. In preliminary tests, first functionality of the TX-RX system and an assessment of the amplitude noise performance of the APD board have been demonstrated. Future work will encompass the completion of the loopback testing as well as the evolution of the testbed towards the targeted milestones.

Acknowledgements

The CLICK mission is a collaboration between the Space, Telecommunications, Astronomy, and Radia-

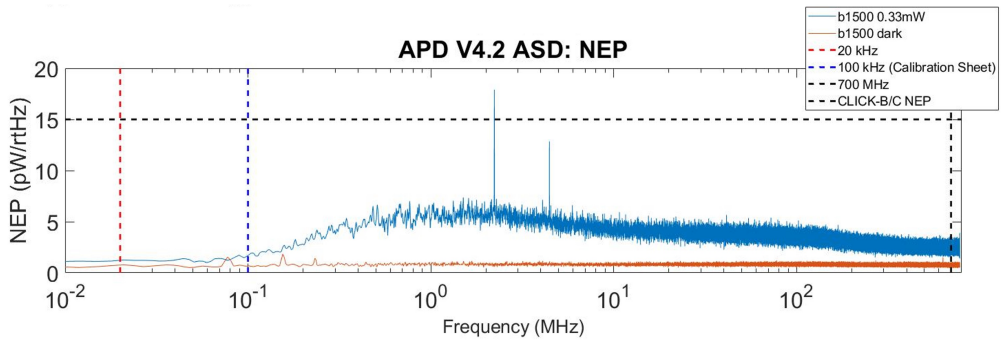

Figure 11: Noise equivalent power of APD board output with and without light impinging.[11]

tion (STAR) Laboratory at the Massachusetts Institute of Technology (MIT), the Precision Space Systems Lab (PSSL) at the University of Florida, CrossTrac Engineering and the NASA Ames Research Center (ARC). The spacecraft are from Blue Canyon Technologies. The CLICK mission is supported by NASA grant 80NSSC18K1579. The views, opinions, and/or findings contained in this work are those of the authors and should not be interpreted as representing the official views or policies, either expressed or implied, of the National Aeronautics and Space Administration.

References

[1] Howard Cannon, Hugo Sanchez, and Dawn M. Mcintosh. "Starling1 - Mission Technologies Overview". In: *Small Sat Conference* (2018).

[2] Kype Leveque et al. "Unlocking the next generation of nano-satellite missions with 320 Mbps KA-band downlink: on-orbit results". In: *Small Sat Conference* (2019).

[3] Stephen Lambert and William Casey. "Laser communications in space". In: *Artech House* (1995).

[4] https://www.jpl.nasa.gov/missions/deep-space-optical-communications-dsoc. *Website*.

[5] C. M. Schieler et al. "TBIRD 200-Gbps CubeSat Downlink: System Architecture and Mission Plan". In: *2022 IEEE International Conference on Space Optical Systems and Applications (ICSOS), Kyoto City, Japan* (2022), pp. 181–185. DOI: 10.1109/ICSOS53063.2022.9749714.

[6] C. M. Schieler et al. "On-orbit demonstration of 200-Gbps laser communication downlink from the TBIRD CubeSat". In: *Free-Space Laser Communications XXXV* 12413 (2023), p. 1241302. DOI: 10.1109/ICSOS53063.2022.9749714.

[7] D.E. Coogan et al. "Development of CubeSat Spacecraft-to-Spacecraft Optical Link Detection Chain for the CLICK-B/C Mission". In: *Small Satellite Conference* (2022).

[8] L. K. Yenchesky. "Optomechanical Design for CubeSat Laser Infrared Crosslinks". Bachelor's Thesis. Massachusetts Institute of Technology, 2019.

[9] William Kammerer et al. "CLICK-A: Optical Communication Experiments from a CubeSat Downlink Terminal". In: *Small Satellite Conference* (2019).

[10] R. Rogalin and M. Srinivasan. "Synchronization for optical PPM with Inter-Symbol Guard Times". In: *IPN Progress Report 42-209* (2017).

[11] D. E. Coogan. "Timing performance simulation, experimentation and analysis for satellite laser time-transfer". PhD thesis. University of Florida, 2023.